MSPR Plenary II - Cellular Signaling and Cardiopulmonary

Thursday, October 8 1:00-2:30 pm CDT

Moderators
David Gordon – University of Iowa
Jennifer Bermick – University of Michigan
Maria Dizon - Ann and Robert H Lurie Children's Hospital of Chicago

CDT	Abstract	Title	Presenting Author
1:00 PM		Introduction & General Information	
1:05 PM	3475730	Eltrombopag inhibits the proliferation of Ewing sarcoma cells via iron chelation and impaired DNA replication.	Torin Waters
1:15 PM	3475772	Percutaneous Closure of Patent Ductus Arteriosus in Very Low Weight Infants: A Meta-Analysis	Adrianne Bischoff
1:25 PM	3475401	A Genetic Model of Diaphragmatic Hernia, Lung Hypoplasia, and Pulmonary Hypertension	Giangela Stokes
1:35 PM	3476303	Effect of postnatal LPS on serum bilirubin levels and markers of systemic and hippocampal inflammation in Gunn rat pups	Katherine Satrom
1:45 PM	3476318	Increased microRNAs 125a and 34c contribute to impaired angiogenesis in a fetal lamb model of persistent pulmonary hypertension of the newborn (PPHN)	Devashis Mukherjee
1:55 PM	3476375	The influence of lox pathway lipid mediators on birth length percentile.	Maranda Thompson
2:05 PM	3474972	Aryl hydrocarbon receptor signaling by indole-3-carbinol attenuates inflammation during necrotizing enterocolitis via CD11c+ immune cell signaling	Lila Nolan
2:15 PM	3476275	Pulmonary artery and lung parenchymal growth following early vs. delayed stent interventions in a swine pulmonary artery stenosis model	Luke Lamers
2:30 PM		Wrap Up	

Note: Schedule subject to change based on presenter availability.

CONTROL ID: 3475730

TITLE: Eltrombopag inhibits the proliferation of Ewing sarcoma cells via iron chelation and impaired DNA replication.

DIGITAL OBJECT IDENTIFIER (DOI):

ABSTRACT STATUS: Sessioned

PRESENTER: Torin Waters

AUTHORS/INSTITUTIONS: T. Waters, K. Goss, S. Koppenhafer, W. Terry, D. Gordon, Pediatric Hematology/Oncology, The University of Iowa Hospitals and Clinics, North Liberty, Iowa, UNITED STATES|

CURRENT CATEGORY: Basic Science

CURRENT SUBCATEGORY: None

ABSTRACT BODY:

Background: Ewing sarcoma is an aggressive bone and soft tissue cancer that occurs primarily in children and young adults. The current therapy for Ewing sarcoma consists of cytotoxic chemotherapy in combination with surgery and/or radiation therapy, which are associated with significant toxicities. There is an unmet need to identify chemotherapeutic agents which are toxic to Ewing sarcoma cells while decreasing treatment-related toxicities

Objective: Our objective was to identify a novel therapeutic approach to improve outcomes in Ewing sarcoma while reducing therapy-related toxicity. We did this by identifying the selective toxicity of eltrombopag toward Ewing sarcoma through the PRISM drug screen. Eltrombopag is an FDA-approved thrombopoietin-receptor agonist (TPO-RA) that is currently being evaluated as a treatment for chemotherapy-induced thrombocytopenia. We aimed to demonstrate the potential benefits of this agent in Ewing sarcoma by confirming this toxicity and investigating its mechanism of action.

Design/Methods: We utilized the Broad Institute's PRISM drug repurposing screen to identify eltromboag's selective toxicity toward Ewing sarcoma cells. We performed cell viability, colony formation assays, and protein immunoblotting to confirm this toxicity. We used Click-iT Edu-488 Kit for flow cyometry and PIP-FUCCI cell imaging to analyze eltrombopag's effects on the cell cycle.

Results: Dose-response assays in 5 Ewing sarcoma cell lines showed IC50s between 2.7 uM and 10.6 uM, comparable to the serum drug level achieved in patients who receive eltrombopag. An osteosarcoma cell line was ~2-5-fold less sensitive to eltrombopag. Colony formation assays showed similar results. Pretreatment with transferrin, a source of biologically availble iron, partially rescued toxicity in several Ewing sarcoma cell lines. Using EdU incorporation assays and PIP-FUCCI cell imaging, we showed that eltrombopag impairs DNA replication in Ewing sarcoma cell lines and increases the number of cells in S phase. Immunoblotting showed that markers of DNA damage (such as gH2AX) were increased, and that tahe CHK1 DNA damage response pathway was activated.

Conclusion(s): In conclusion, our data suggest that eltrombopag, a well-tolerated drug used to treat pediatric chronic ITP and aplastic anemia, could provide therapeutic benefit for patients with Ewing sarcoma by both mitigating treatment-related thrombocytopenia and contributing additional anti-tumor toxicity via iron chelation and RNR inhibition.

(no table selected)

IMAGE CAPTION: Eltrombopag inhibits Ewing sarcoma growth *in vitro*. (A) Dose response curves for Ewing sarcoma and osteosarcoma (U2OS) cell lines treated with different concentrations of eltrombopag. Cell viability was assessed 72 h after drug was added. Error bars represent the mean ± SD of three technical replicates. (B-C) Colony formation assay for (B) Ewing sarcoma and (C) osteosarcoma cell lines treated with eltrombopag 5 mM for 14 days. Eltrombopag causes DNA damage and activates the CHK1 pathway in Ewing sarcoma cells. (A-C) Ewing sarcoma cell lines were treated with eltrombopag 5 mM or vehicle for 18 hours. Cells were then labeled with EdU and fixed for flow cytometry for gH2AX, a marker of DNA damage. (D) Ewing sarcoma cell lines were treated with eltrombopag as described in (A) and then cellular lysates were collected for immunoblotting.

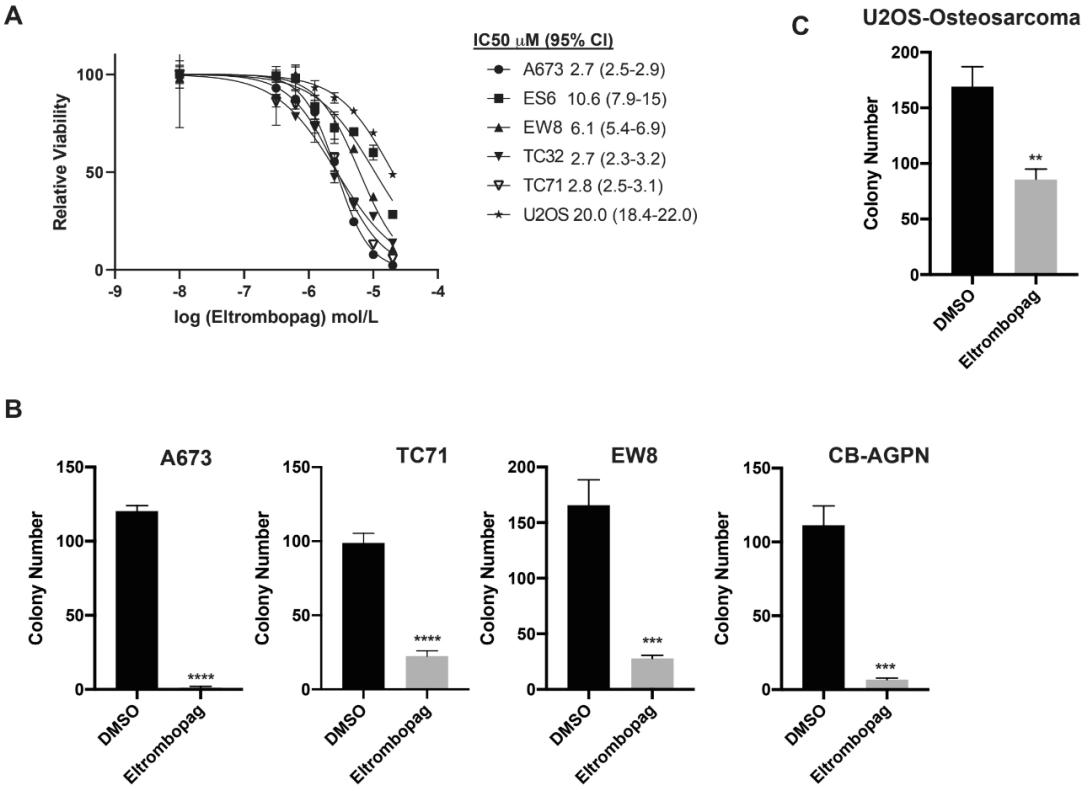

Eltrombopag inhibits Ewing sarcoma growth *in vitro*. (A) Dose response curves for Ewing sarcoma and osteosarcoma (U2OS) cell lines treated with different concentrations of eltrombopag. Cell viability was assessed 72 h after drug was added. Error bars represent the mean ± SD of three technical replicates. (B-C) Colony formation assay for (B) Ewing sarcoma and (C) osteosarcoma cell lines treated with eltrombopag 5 mM for 14 days.

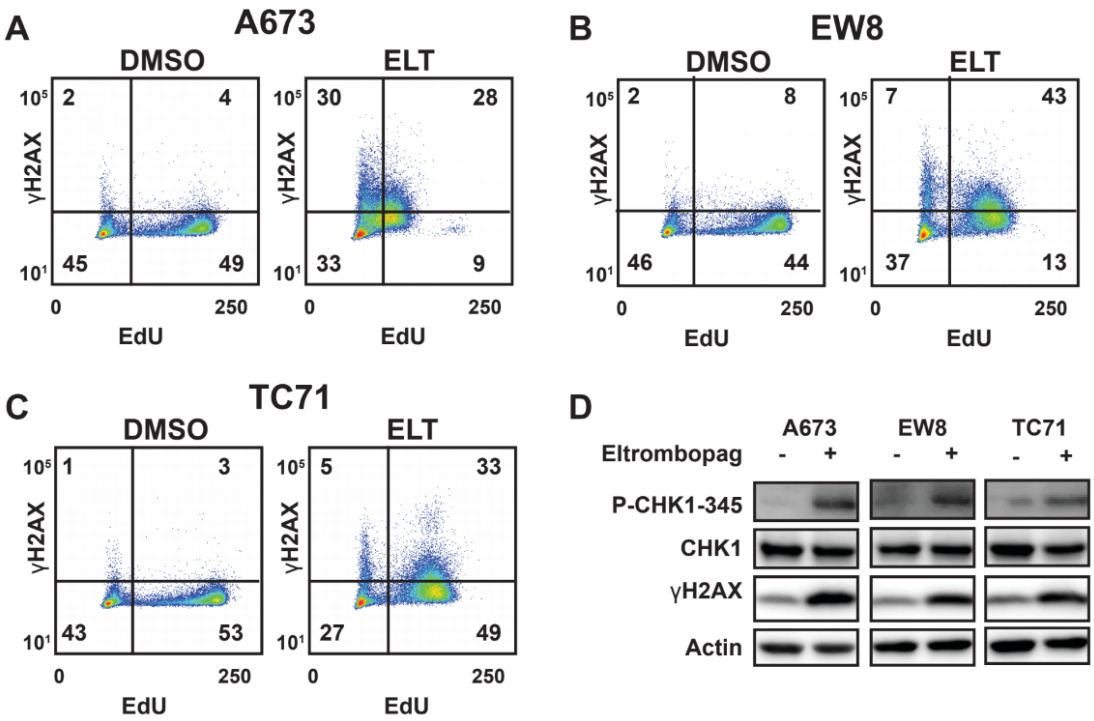

Eltrombopag causes DNA damage and activates the CHK1 pathway in Ewing sarcoma cells. (A-C) Ewing sarcoma cell lines were treated with eltrombopag 5 mM or vehicle for 18 hours. Cells were then labeled with EdU and fixed for flow cytometry for gH2AX, a marker of DNA damage. (D) Ewing sarcoma cell lines were treated with eltrombopag as described in (A) and then cellular lysates were collected for immunoblotting.

CONTROL ID: 3475772

TITLE: Percutaneous Closure of Patent Ductus Arteriosus in Very Low Weight Infants: A Meta-Analysis

DIGITAL OBJECT IDENTIFIER (DOI):

ABSTRACT STATUS: Sessioned

PRESENTER: Adrianne Rahde Bischoff

AUTHORS/INSTITUTIONS: A.R. Bischoff, P. McNamara, Pediatrics, University of Iowa, Iowa City, Iowa, UNITED STATES|B. Jasani, Pediatrics, The Hospital for Sick Children, Toronto, Ontario, CANADA|S. Sathanandam, Pediatrics, The University of Tennessee Health Science Center, Memphis, Tennessee, UNITED STATES|C. Backes, Pediatrics, Nationwide Children's Hospital, Columbus, Ohio, UNITED STATES|D. Weisz, Newborn and Developmental Paediatrics, Sunnybrook Health Sciences Centre, Toronto, Ontario, CANADA|

CURRENT CATEGORY: Clinical Investigation

CURRENT SUBCATEGORY: None

ABSTRACT BODY:

Background: Patent ductus arteriosus (PDA) is associated with significant morbidity in neonates, particularly preterm infants. Percutaneous (catheter-based) closure is the procedure of choice for adults and older children with a patent ductus arteriosus (PDA). The practice of device closure in lower weight infants is becoming more common but data on clinical efficacy and safety are limited.

Objective: To investigate technical success and safety of percutaneous PDA closure in very low weight (VLW=<1.5kg) infants.

Design/Methods: The study was performed according to the Systematic Reviews and Meta-Analysis checklist and was registered prospectively (PROSPERO). Data sources used included Scopus, Web of Science, Embase, CINAHL, Cochrane, PubMed searched from inception to April 2020 with no language restrictions. Study selection included publications with a clear definition of the intervention as percutaneous PDA closure in VLW infants. Data extraction was independently performed by multiple observers. Primary outcome was technical success and secondary outcomes were adverse events (AE). Subgroup analysis was performed in infants <6kg. Data were pooled by using a random-effects model

Results: Twenty-eight studies, including 373 infants <1.5kg and 69 studies enrolling 1794 infants <6kg were included. In patients <1.5kg, technical success was 96% (95% CI 93-98%, p=0.16, I2 =23%). Mean age and weight at the time of the procedure were 29.5±14.4 days and 1060±238 grams, respectively. Overall incidence of AE was 27% (95% CI 17-38%, p<0.001, I2=70%) and clinically significant AEs was 8% (95% CI 5-10%, p=0.63, I2=0%). The probability of technical failure was inversely related to age at the time of the procedure [OR 0.9 (95% CI 0.830-0.974), p=0.009]. A trend towards increased estimated probability of success according to year of publication/procedure [OR 1.212 (95% CI 0.985-1.493), p=0.069] was noted, despite progressive reduction in procedural weight over time. Infants <6kg had technical success of 93% (95% CI 91-95%, p<0.001, I2=50%), AE of 25% (95% CI 20-31%, p<0.001, I2 =82%) and CS-AE of 10% (95% CI 7-12%, p<0.001, I2=54%).

Conclusion(s): Percutaneous PDA closure is feasible and associated with a limited clinically significant and catastrophic AEs in VLW infants. Procedural success has increased over time despite progressive increases in number of procedures performed in smaller and younger patients. Age at the time of the procedure has a significant impact on technical success and should be taken into consideration for decision-making.

(no table selected)

IMAGE CAPTION: Forest plot of frequency of technical success of percutaneous PDA closure among infants ≤1.5kg. Probability of technical failure of percutaneous PDA closure in neonates ≤1.5kg according to age at the time of the procedure.

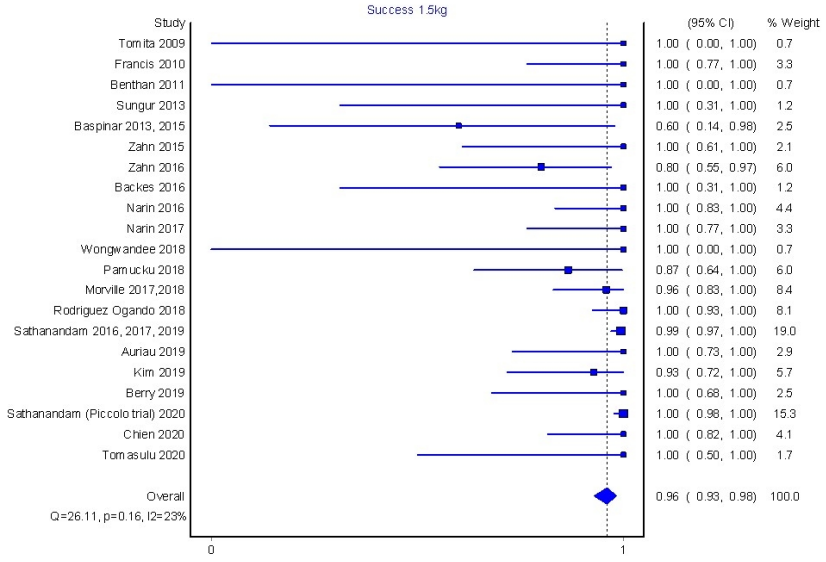

Forest plot of frequency of technical success of percutaneous PDA closure among infants ≤1.5kg.

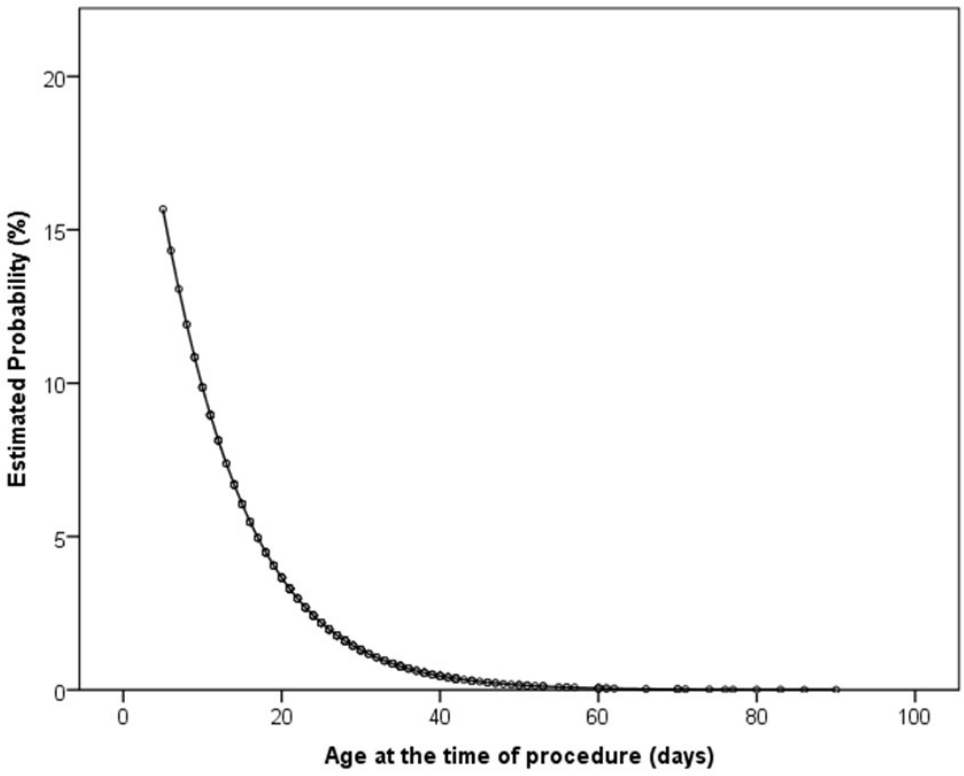

Probability of technical failure of percutaneous PDA closure in neonates ≤1.5kg according to age at the time of the procedure.

CONTROL ID: 3475401

TITLE: TITLE: A Genetic Model of Diaphragmatic Hernia, Lung Hypoplasia, and Pulmonary Hypertension

DIGITAL OBJECT IDENTIFIER (DOI):

ABSTRACT STATUS: Sessioned

PRESENTER: Giangela Maria Stokes

AUTHORS/INSTITUTIONS: G.M. Stokes, W. Genthe, M. Brix, D.J. McCulley, Department of Pediatrics, University of Wisconsin-Madison, Madison, Wisconsin, UNITED STATES|

CURRENT CATEGORY: Basic Science

CURRENT SUBCATEGORY: None

ABSTRACT BODY:

Background: Background: Congenital diaphragmatic hernia (CDH) is a common and severe congenital malformation, affecting 1 in 3500 live births with a mortality rate of 20-50%. The high mortality is due to failure of lung and pulmonary vascular development causing a frequently lethal combination of lung hypoplasia and pulmonary hypertension. The severity of these defects is highly variable and their developmental origins are unclear. Our hypothesis is that a core group of genes is required for both diaphragm formation and development of the lungs and pulmonary vasculature. Mutations in these genes or disruption of their downstream signals may be responsible for lung hypoplasia and pulmonary hypertension. Using genome sequencing, mutations in the SIN3A gene have been identified in patients with CDH; however, the role that SIN3A plays in diaphragm, lung, or pulmonary vascular development is not clear.

Objective: Objective: To determine the role of Sin3a in the developing diaphragm and lung mesenchyme and identify the developmental mechanisms responsible for lung hypoplasia pulmonary hypertension due to Sin3a loss of function.

Design/Methods:

Design/Methods: Using a tissue-specific, conditional knockout approach in a mouse model, we inactivated the expression of Sin3a in the developing diaphragm or lung mesenchyme. We used a combination of histology, gene expression analysis, and physiology to analyze the phenotype.

Results: Results: Deletion of Sin3a in the diaphragm mesothelium or skeletal muscle resulted in failure of diaphragm formation and CDH in mice. Furthermore, deletion of Sin3a in the lung mesenchyme alone resulted in lung hypoplasia and pulmonary hypertension in the absence of CDH, due to defects in cell proliferation and differentiation. RNA-seq analysis of recombined embryonic lung mesenchymal cells revealed many differentially expressed genes are normally expressed in lung progenitor populations. The majority of these differentially expressed genes regulate inflammation, cell cycle regulation, rRNA processing, and metabolism.

Conclusion(s): Conclusion(s): Mutations in the SIN3A gene result in human CDH. Tissue-specific deletion of Sin3a in a mouse model results in lung hypoplasia and pulmonary hypertension. Sin3a is required for normal cell proliferation, survival, and differentiation during lung and pulmonary vascular development. These data support the model that genetic defects in patients with CDH can cause abnormal development of the lung and pulmonary vasculature independent of the associated diaphragm defect.

(no table selected)

(No Image Selected)

CONTROL ID: 3476303

TITLE: Effect of postnatal LPS on serum bilirubin levels and markers of systemic and hippocampal inflammation in Gunn rat pups

DIGITAL OBJECT IDENTIFIER (DOI):

ABSTRACT STATUS: Sessioned

PRESENTER: Katherine Satrom

AUTHORS/INSTITUTIONS: K. Satrom, G. Singh, Pediatrics, University of Minnesota, Minneapolis, Minnesota, UNITED STATES|T. Gisslen, University of Minnesota System, Minneapolis, Minnesota, UNITED STATES|

CURRENT CATEGORY: Basic Science

CURRENT SUBCATEGORY: None

ABSTRACT BODY:

Background: Unconjugated hyperbilirubinemia (UCB) and postnatal infections are common co-morbidities in extremely preterm infants. Severe UCB leads to neuronal injury, including in the hippocampus (HPC). Whether infection-induced inflammation worsens HPC injury by exaggerating UCB is not known. UCB is also an antioxidant and may protect against systemic and/or neuronal-specific inflammation.

Objective: Determine the effects of LPS-induced inflammation on serum bilirubin levels and markers of systemic and hippocampal inflammation in Gunn rat pups.

Design/Methods: Gunn rat pups were exposed to either LPS (0.075 mg/kg ip) or saline (sal) on postnatal day 5 (P5, similar to 28 wk preterm human brain). Homozygous Gunn rat pups (jj) develop neonatal UCB due to a UDP-GT mutation, while the heterozygous (Nj) pups remain unaffected. On P7, serum was collected for total bilirubin (TSB) and cytokine quantification from Nj+sal, Nj+LPS, jj+sal, and jj+LPS groups (n=6-8/group).The cytokine mRNA transcript expression in the HPC was determined using qPCR. Groups were compared using one-way ANOVA with Tukey's multiple comparison test.

Results: Mean (±SEM) TSB levels were higher in jj+LPS (9.3 ± 0.25 mg/dL) compared with jj+sal (6.8 ± 0.26 mg/dL) group, $p<0.01$. Serum IL-10 (+ 236%; $p<0.01$) and IL-1b (+ 213%; $p=0.11$) levels were higher in the Nj+LPS group compared with the Nj+sal group, but not in the jaundiced group (jj+LPS vs. jj+sal) despite higher TSB levels in jj+LPS group. HPC transcript expression of IL-10 was decreased in jj+LPS compared with jj+sal (-52%, $p<0.05$) but not in Nj+LPS vs. Nj+sal. TGF-b2 HPC transcript expression was significantly upregulated in Nj+LPS vs. Jj+sal (+64%; $p<0.05$) but not in jj+LPS vs. jj+sal.

Conclusion(s): LPS exacerbated UCB in jaundiced Gunn rat pups, but not systemic and hippocampal-specific inflammation. Bilirubin's innate antioxidant effect may be responsible for the suppression of cytokine expression in the hippocampus.

(no table selected)

(No Image Selected)

CONTROL ID: 3476318

TITLE: Increased microRNAs 125a and 34c contribute to impaired angiogenesis in a fetal lamb model of persistent pulmonary hypertension of the newborn (PPHN)

DIGITAL OBJECT IDENTIFIER (DOI):

ABSTRACT STATUS: Sessioned

PRESENTER: Devashis Mukherjee

AUTHORS/INSTITUTIONS: D. Mukherjee, U. Rana, T. Michalkiewicz, G.G. Konduri, Neonatology, Medical College of Wisconsin, Milwaukee, Wisconsin, UNITED STATES|A. Kriegel, Physiology, Medical College of Wisconsin, Milwaukee, Wisconsin, UNITED STATES|

CURRENT CATEGORY: Basic Science

CURRENT SUBCATEGORY: None

ABSTRACT BODY:

Background: MicroRNAs (miRs) are conserved, short, noncoding nucleotide strands. They bind to the mRNA 3' untranslated region and degrade mRNA or repress translation, altering gene expression. In PPHN, pulmonary vascular pressures fail to decrease after birth. Decrease in angiogenesis contributes to PPHN; mechanisms remain unclear.

Objective: To identify differential expression of miRs in a ductal ligation lamb model of PPHN using next generation sequencing (NGS) and study the angiogenesis effects of altered miR expression in pulmonary artery endothelial cells (PAECs) in vitro.

Design/Methods: PPHN was induced by prenatal ductus arteriosus ligation. Small RNA libraries constructed from PAEC RNA from PPHN and control lambs was used for NGS to identify miRs differentially expressed in PAECs. TargetScan® was used to identify mRNA targets. MiRs having the strongest baseline PAEC expression, significant fold change in PPHN and predicted targets in angiogenesis signaling pathways were selected for study. PAECs were transfected with miR mimics and anti-miRs and harvested at 48 h for immunoblotting, PCR and angiogenesis assays (cell count, migration, tube formation). All tests were performed first in human umbilical vein endothelial cells (HUVECs) to standardize transfection protocol.

Results: We identified 470 miRs; 12 were significantly differentially expressed between control and PPHN PAECs ($p < 0.05$, adjusted for multiple comparisons). miR-125a and miR-34c were significantly up-regulated in PPHN vs control ($p=0.003$ for miR-125a, $p=0.02$ for miR-34c) and have targets in the angiogenesis pathway. Transfection of control fetal lamb PAEC with miR-125a and miR-34c mimics separately decreased capillary tube formation in Matrigel in vitro. Tube formation was impaired in PPHN PAECs at a baseline, compared to control PAECs. Transfection of PPHN PAECs with anti-miR125a and anti-miR34c separately, improved the tube formation by these PAECs (Table 1). HUVECs showed similar results along with decreased cell count and migration (Table 2). Successful transfection was verified by PCR fold change in transfected HUVECs using human miR primers.

Conclusion(s): Both miR-34c and miR-125a are increased in PPHN lamb PAECs. They impair angiogenesis in control PAECs and their inhibition improves angiogenesis in PPHN cells. Finding their mRNA targets will help identify key angiogenesis regulators and develop novel therapeutic strategies.

(no table selected)

IMAGE CAPTION:

	Control PAEC + control miR mimic	Control PAEC + miR-34c mimic	Control PAEC + miR-125a mimic
Number of nodes (per hpf)	447	22	28.5
Number of meshes (per hpf)	16	1	0
Total branching length (pixels per hpf)	16009	1362	1390
	PPHN PAEC + control anti-miR	PPHN PAEC + anti-miR-34c	PPHN PAEC + anti-miR-125a
Number of nodes (per hpf)	68	267	214
Number of meshes (per hpf)	3	26.5	13
Total branching length (pixels per hpf)	4113	12168	5361

Table 1: Capillary tube formation assay for control PAECs transfected with miR mimics and PPHN PAECs transfected with antimiRs. All results were significant for $p<0.05$. hpf : high power field, PAEC : pulmonary artery endothelial cell, PPHN : persistent pulmonary hypertension of the newborn, miR: microRNA

Cell count (10^5) with seeding density of 1 X 10^5		HUVEC + control miR	HUVEC + miR-34c	p = 0.04
		7.1	5.1	
		HUVEC + control miR	HUVEC + miR-125a	p = 0.05
		5.1	3.5	
Width of scratch after 5 h (um)		HUVEC + control miR	HUVEC + miR-34c	p = 0.002
		444.8	664.0	
		HUVEC + control miR	HUVEC + miR-125a	p = 0.0002
		431.8	685.8	
Capillary tube formation assay using Matrigel	Number of Nodes (per hpf)	HUVEC + control miR	HUVEC + miR-34c	p = 0.003
		1547	117	
		HUVEC + control miR	HUVEC + miR-125a	p = 0.01
		1547	401	
	Number of meshes (per hpf)	HUVEC + control miR	HUVEC + miR-34c	p = 0.02
		146	3	
		HUVEC + control miR	HUVEC + miR-125a	p = 0.01
		146	15	
	Total branching length (pixels per hpf)	HUVEC + control miR	HUVEC + miR-34c	p = 0.0003
		44881	6177	
		HUVEC + control miR	HUVEC + miR-125a	p = 0.06
		44881	18363	

Table 2: Angiogenesis assay results from transfection of HUVECs with control miRs, miR-34c and miR-125a mimics separately. All tests were performed at 48h after transfection. hpf: high power field, HUVEC: human umbilical vein endothelial cell, miR: microRNA.

CONTROL ID: 3476375

TITLE: THE INFLUENCE OF LOX PATHWAY LIPID MEDIATORS ON BIRTH LENGTH PERCENTILE.

DIGITAL OBJECT IDENTIFIER (DOI):

ABSTRACT STATUS: Sessioned

PRESENTER: Maranda Thompson

AUTHORS/INSTITUTIONS: M. Thompson, M. VanOrmer, Pediatrics, University of Nebraska Medical Center, Omaha, Nebraska, UNITED STATES|A. Anderson Berry, M. Thoene, Pediatrics, University of Nebraska Medical Center College of Medicine, Omaha, Nebraska, UNITED STATES|A. Ulu, T. Nordgren, Biomedical Sciences, University of California Riverside, Riverside, California, UNITED STATES|C. Hanson, Allied Health Professions, University of Nebraska Medical Center, Omaha, Nebraska, UNITED STATES|A. Yuil-Valdes, Pathology, University of Nebraska Medical Center, Omaha, Nebraska, UNITED STATES|S. Natarajan, Nutrition and Health Sciences, University of Nebraska System, Lincoln, Nebraska, UNITED STATES|M. Mukherjee, Allied Health Professions, University of Nebraska Medical Center, Omaha, Nebraska, UNITED STATES|

CURRENT CATEGORY: Clinical Investigation

CURRENT SUBCATEGORY: None

ABSTRACT BODY:

Background: Fatty acids have key roles in regulating physiological processes and can exert their effects through their enzymatic breakdown into bioactive metabolites. Linoleic acid (LA, n-6) and alpha-linolenic acid (ALA, n-3) are essential fatty acids that give rise to arachidonic acid (ARA, n-6) a pro-inflammatory eicosanoids, and the anti-inflammatory eicosanoids eicosapentaenoic acid (EPA, n-3) and docosahexaenoic acid (DHA, n-3). In pregnancy, n-3 fatty acids are important for maternal and fetal health, but little is known about the influence of lipoxygenase (LOX) enzymatic pathway metabolite levels in maternal and cord plasma on infant outcomes.

Objective: The objective of this study was to determine the association between maternal and cord plasma LOX metabolite levels and birth outcomes.

Design/Methods: This study was conducted in a Midwest medical center on the Labor and Delivery floor. Eligibility for participation in the study included, mothers receiving prenatal care and planning on delivering at Nebraska Medicine, live pregnancy, and maternal-infant pairs free of renal, metabolic or hepatic disease that impair normal nutrient metabolism. Maternal and umbilical cord plasma were collected at the time of delivery and metabolite levels were analyzed using lipid chromatography tandem-mass spectrometry. Spearman correlation coefficients were used to assess associations between continuous variables. Linear regression modelling was performed on metabolites correlated with birthweight percentile and adjusted for obesity (>30 or <= 30 BMI) and maternal smoking status (current/former vs. never) in the models. Metabolites were log-transformed in the regression analyses to meet the statistical assumptions of the models. $P<0.05$ was considered statistically significant.

Results: Maternal-infant pairs demonstrated significant differences in metabolite levels between maternal and cord plasma, with certain cord metabolite levels significantly predicting birth length percentage. Figure 1 demonstrates metabolites that significantly differed or approached significance between maternal and cord plasma levels. Figure 2 demonstrates the specific LOX metabolites significantly associated with birth length percentile after adjusting for maternal obesity and smoking. For example, Cord 13-HODE is predictive of birth length percentage ($p=0.0056$) and for every 1% increase in cord plasma levels, the expected mean birth length percentile increases by 0.21.

Conclusion(s): LOX pathway metabolite levels at the time of delivery was predicitive of birth length percentage.

(no table selected)

IMAGE CAPTION: Table 1 demonstrates the levels of metabolites in maternal and cord plasma that were significantly different or approached significance. Spearman correlations were used to assess the association between metabolite levels in maternal and cord plasma at the time of delivery. Non-significant relationships were not included. Table 2 illustrates the LOX metabolites that were significantly predictive of birth outcomes after adjusting for maternal obesity and smoking status. Linear regression modelling was performed on metabolites correlated with birthweight percentile, birth length percentile or birth head circumference percentile at the $p<0.05$ level on univariate analysis. LOX metabolites were only significantly correlated with birth length percentile.

Table 1: Significant Spearman correlations between LOX Pathway metabolite levels in maternal and cord plasma at the time of delivery

LOX Pathway Metabolites		(n)	Mean (pg/ml)	Standard Deviation	Median	Minimum	Maximum	Quartile Range	Rho (p-value)
Arachidonic Acid (AA) Metabolites									
5-HETE	Maternal	78	46.60	171.0	7.970	0.4500	1202	12.52	0.4074 (<0.001)
	Cord	76	11.10	16.60	7.800	0.8000	111.2	4.870	
8-HETE	Maternal	78	3.130	7.250	1.330	0.1800	50.22	1.730	0.365 (0.0016)
	Cord	76	2.350	2.120	1.840	0.7300	15.99	1.140	
9-HETE	Maternal	77	3.240	8.340	1.070	0.1100	56.25	1.530	0.254 (0.03)
	Cord	76	2.550	1.950	2.200	0.5900	13.07	1.530	
11-HETE	Maternal	78	4.670	11.16	1.930	0.1200	75.44	2.210	0.371 (0.0013)
	Cord	76	3.650	5.290	2.350	0.7400	44.90	1.850	
12-HETE	Maternal	78	6.070	9.400	3.470	0.1800	58.30	4.340	0.236 (0.046)
	Cord	76	79.44	386.2	8.150	1.200	3240	12.33	
15-HETE	Maternal	77	2.770	2.830	2.080	0.04000	12.65	3.510	0.513 (<0.001)
	Cord	76	4.920	4.020	4.200	0.1100	21.16	4.050	
Lipoxin A4**	Maternal	65	42.53	126.6	8.720	1.360	777.3	13.41	0.250 (0.058)
	Cord	67	9.080	11.44	5.840	1.140	77.16	4.070	
Linoleic Acid (LA) Metabolites									
13-HODE**	Maternal	78	32.41	40.16	21.07	6.730	228.9	15.36	0.206 (0.08)
	Cord	76	13.34	7.240	12.00	3.940	40.67	8.520	
Alpha Linoleic Acid (ALA) Metabolites									
15-HETrE**	Maternal	78	1.640	4.090	0.6900	0.1100	31.85	0.7500	0.19733 (0.0966)
	Cord	76	1.730	1.510	1.370	0.5000	11.60	0.8700	
Eicosapentaenoic Acid (EPA) Metabolites									
5-HEPE	Maternal	77	1.490	4.660	0.4300	0.1000	33.71	0.5300	0.37476 (0.0013)
	Cord	76	0.4800	0.4600	0.3900	0.1000	2.960	0.2400	
9-HEPE	Maternal	47	0.2300	0.4100	0.1100	0.0	2.460	0.1400	0.41175 (0.0113)
	Cord	47	0.1000	0.08000	0.08000	0.01000	0.5400	0.0600	
12-HEPE	Maternal	67	0.2400	0.4900	0.09000	0.02000	2.960	0.1600	0.59806 (<.0001)
	Cord	74	1.280	6.240	0.1100	0.02000	52.49	0.2100	
5,15-DiHETE	Maternal	53	2.820	10.28	0.1700	0.02000	61.74	0.2700	0.32671 (0.0325)
	Cord	64	0.3300	0.7700	0.1300	0.03000	5.600	0.1300	
Docosahexaenoic Acid (DHA) Metabolites									
7-HDHA	Maternal	63	2.800	6.850	1.100	0.2000	46.28	1.170	0.36722 (0.0042)
	Cord	75	1.040	0.8900	0.7800	0.2400	6.960	0.7200	
17-HDHA	Maternal	59	2.080	2.170	1.430	0.02000	9.090	2.700	0.49534 (0.0003)
	Cord	66	2.090	1.660	1.830	0.1000	11.47	1.280	

** indicates correlations that approached significance

Table 1 demonstrates the levels of metabolites in maternal and cord plasma that were significantly different or approached significance. Spearman correlations were used to assess the association between metabolite levels in maternal and cord plasma at the time of delivery. Non-significant relationships were not included.

Table 2: Birth length percentile significantly correlated with LOX pathway metabolites after adjustment for maternal obesity and smoking status.			
Birth Length Percentile	**(n)**	**Parameter Estimate**	**p-value**
Cord 13-HODE	73	0.21	0.0056
Cord 13-KODE	73	0.16	0.037
Cord 5-HEPE	73	0.14	0.017
Cord 7-HDHA	72	0.16	0.0086

Table 2 illustrates the LOX metabolites that were significantly predictive of birth outcomes after adjusting for maternal obesity and smoking status. Linear regression modelling was performed on metabolites correlated with birthweight percentile, birth length percentile or birth head circumference percentile at the $p<0.05$ level on univariate analysis. LOX metabolites were only significantly correlated with birth length percentile.

CONTROL ID: 3474972

TITLE: Aryl hydrocarbon receptor signaling by indole-3-carbinol attenuates inflammation during necrotizing enterocolitis via CD11c+ immune cell signaling

DIGITAL OBJECT IDENTIFIER (DOI):

ABSTRACT STATUS: Sessioned

PRESENTER: Lila S. Nolan

AUTHORS/INSTITUTIONS: L.S. Nolan, B. Mihi, Q. Gong, J. Rimer, S. Gale, M. Goree, E. Hu, W. Lanik, A. Lewis, M. Good, Newborn Medicine, Washington University in Saint Louis School of Medicine, Saint Louis, Missouri, UNITED STATES|P. Agrawal, V. Liu, A. Bustos, Washington University in Saint Louis, Saint Louis, Missouri, UNITED STATES|Z. Hodzic, Medicine, University of Pittsburgh Medical Center, Pittsburgh, Pennsylvania, UNITED STATES|M. Laury, Genome Technology Access Center, McDonnell Genome Institute, Washington University in Saint Louis School of Medicine, Saint Louis, Missouri, UNITED STATES|

CURRENT CATEGORY: Basic Science

CURRENT SUBCATEGORY: None

ABSTRACT BODY:

Background: Necrotizing enterocolitis (NEC) is a significant cause of morbidity and mortality in preterm infants. The identification of preventative strategies against NEC remains a priority. The aryl hydrocarbon receptor (AhR) has an established role in the homeostasis of intestinal immune function, though its role in NEC is unknown.

Objective: To determine the role of AhR activation in a murine model of NEC.

Design/Methods: Experimental NEC was induced in four-day-old wild-type (WT) mice or mice selectively lacking AhR expression in the intestinal epithelial cells ($AhR^{\Delta IEC}$) or in $CD11c^{+}$ cells ($AhR^{\Delta CD11c}$) with twice daily hypoxic stress and gavage feeding with formula supplemented with lipopolysaccharide and enteric bacteria. Control mice were dam-fed. WT pups subjected to NEC received either enteral AhR ligand, indole-3-carbinol (I3C), resuspended in corn oil dosed 50 µg/g twice daily or corn oil alone (vehicle). Animals were euthanized and terminal ileum was collected at 72 hours for analysis.

Results: Enteral I3C supplementation attenuated the inflammatory response in WT pups with experimental NEC as shown by downregulated expression of Il-1β (P=0.0015) and macrophage scavenger receptor MARCO (P=0.0197) when compared to pups with NEC receiving vehicle alone. Transcriptional and enrichment pathway analyses in pups with NEC receiving I3C indicated decreased gene expression in nucleotide-binding and oligomerization domain (NOD)-like receptor signaling, a pathway involved in intestinal mucosal injury during NEC. $AhR^{\Delta IEC}$ pups exhibited a similar susceptibility to experimental NEC compared with WT littermates. $AhR^{\Delta CD11c}$ pups with NEC demonstrated increased inflammation, with increased Il-1β expression in the terminal ileum (P=0.0006) compared to WT. To identify mechanisms mediating the increased inflammatory response in $AhR^{\Delta CD11c}$ mice, lamina propria cells were isolated for flow cytometry and exhibited an increase in $Tim\text{-}4^{-}$ monocyte-dependent subset of macrophages in $AhR^{\Delta CD11c}$ pups compared with WT.

Conclusion(s): I3C attenuates intestinal inflammation during experimental NEC via $CD11c^{+}$ immune cell signaling, whereas AhR signaling in intestinal epithelial cells is dispensable in NEC. Importantly, this data suggests that ileal Il-1β expression during NEC in $AhR^{\Delta CD11c}$ pups is likely driven by the $Tim\text{-}4^{-}$ intestinal macrophage subset. Further, AhR ligands may be an innovative therapeutic in managing this devastating disease.

(no table selected)

(No Image Selected)

CONTROL ID: 3476275

TITLE: Pulmonary artery and lung parenchymal growth following early vs. delayed stent interventions in a swine pulmonary artery stenosis model

DIGITAL OBJECT IDENTIFIER (DOI):

ABSTRACT STATUS: Sessioned

PRESENTER: Luke Lamers

AUTHORS/INSTITUTIONS: R. Pewowaruk, A. Roldan-Alzate, Biomedical Engineering, University of Wisconsin-Madison, Madison, Wisconsin, UNITED STATES|L. Lamers, Pediatrics Division of Cardiology, University of Wisconsin-Madison, Madison, Wisconsin, UNITED STATES|

CURRENT CATEGORY: Basic Science

CURRENT SUBCATEGORY: None

ABSTRACT BODY:

Background: From birth to 3-5 years age there is rapid increase in alveoli and pulmonary vessels. Branch pulmonary artery stenosis (PAS) early in life alters pulmonary blood flow (PBF) during this critical period. How the pulmonary circulation remodels in response to different durations low PBF and how much growth can be recovered with different interventions timings are unknown.

Objective: Use a pig PAS model to test if early stent interventions to restore PBF during alveolar and PA development is superior to later stenting when PA multiplication is not possible.

Design/Methods: In 14 piglets, left PAS (LPAS) was surgically created. Five had early stent intervention (EI group) at 5 weeks age in the alveolar multiplication period with stent dilation at 10 weeks of age. Five had delayed stent intervention (DI group) at 10 weeks age near the end of the alveolar multiplication period. Four served as LPAS and four as sham controls. All had catheterization, imaging and histology at 20 weeks age. Statistical analysis used non-parametric tests.

Results: At the 20 week catheterization, LPAS had increased RV and MPA pressures. Both DI and EI normalized RV/PA pressures with no differences between the two. L lung PBF decreased from 52±5% in shams to 7±2% in LPAS ($p<0.01$). EI and DI improved but did not normalize L lung PBF (44±3% and 40±2% EI vs DI).

DI and EI improved the proximal LPA size (stent) vs LPAS (1.4±0.1 mm) but was decreased vs sham (15.2±0.8 mm) for DI (10.0±0.8 mm) and EI (10.4±0.5 mm). The distal LPA and LPA segmental branch size was similar for EI vs DI and greater than LPAS.

The ratio of the L/total lung volume from CT was 39±2% in shams and 30±1% in LPAS ($p<0.01$). EI trended towards increased L lung volume ratio at 36±3% ($p=0.07$ vs LPAS) compared to 34±2% in DI ($p=0.87$ vs LPAS).

While not statistically significant, EI and sham trended towards greater L lung alveoli density vs LPAS and DI. LPAS and DI had L lung alveolar septal and bronchovascular abnormalities vs sham ($p<0.05$), that were minor in EI.

Conclusion(s): In this swine PAS model, early interventions improved lung parenchyma anatomy but not PA growth, hemodynamics or PBF to delayed interventions. These data suggest that lung reperfusion during the rapid alveolar multiplication period improves lung parenchyma growth. Further research is required to understand both how these results relate to human patients and the underlying pathophysiology of the lung response to PAS and current interventional therapies.

(no table selected)

IMAGE CAPTION: Figure 1: Study timeline Figure 2: 3D reconstructions of PA anatomy, proximal LPA diameter, main LPA diameters and LPA 1st order branch diameters. Sham (n=4), LPAS (n=4), DI (n=5) and EI (n=5). * $p<0.05$ vs sham control, $^{\#}$ $p<0.05$ vs LPAS control Table 1: Hemodynamics and PBF at 20-weeks for all groups
 Table 2: Left lung histopathology

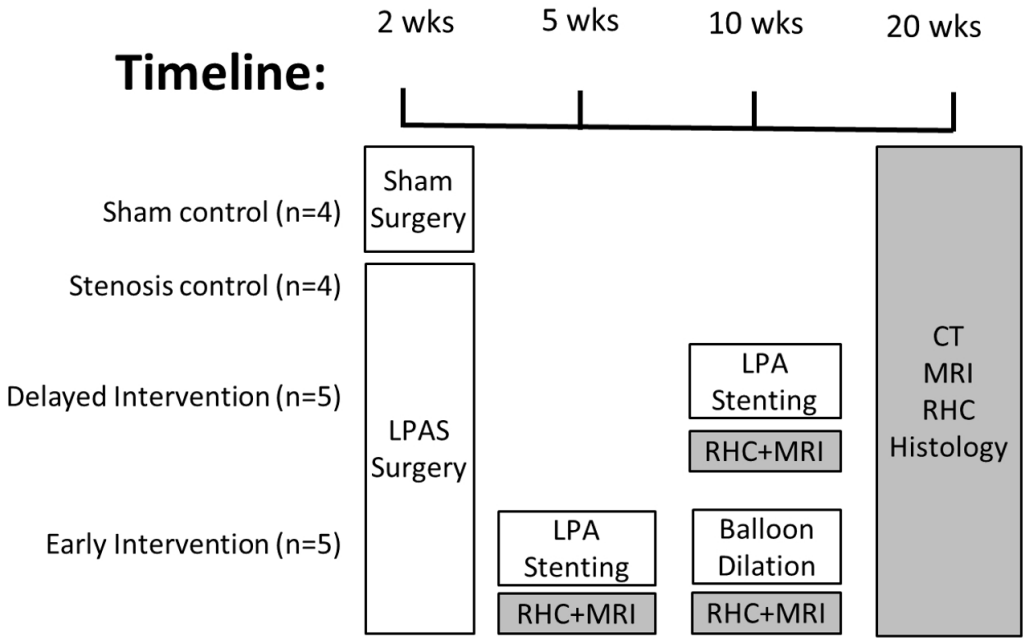

Figure 1: Study timeline

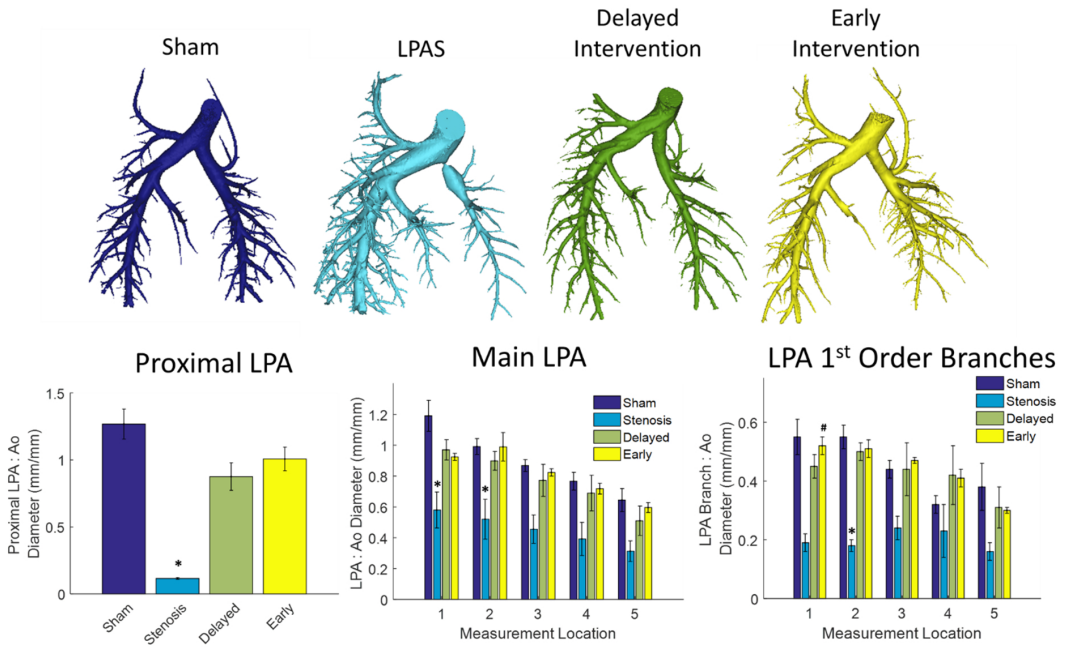

Figure 2: 3D reconstructions of PA anatomy, proximal LPA diameter, main LPA diameters and LPA 1st order branch diameters. Sham (n=4), LPAS (n=4), DI (n=5) and EI (n=5). * p<0.05 vs sham control, $^{\#}$ p<0.05 vs LPAS control

Table 1: Hemodynamics and PBF at 20-weeks for all groups

	Sham (n=4)	LPAS (n=4)	Delayed Intervention (n=5)	Early Intervention (n=5)
BW (kg)	56±3	57±2	59±3	48±5
HR (BPM)	84±4	83±2	105±6	96±8
Fulton Index (g/g)	0.42±0.02	0.40±0.02	0.44±0.02	0.40±0.02
CI (L/min/m^2)	2.8±0.2	3.2±0.1	3.7±0.4	3.6±0.3
L Lung Perfusion (%)	52±5	7±2*	44±3 (n=4)	40±2
Mean RA Pressure (mmHg)	7±2	10±1	6±1	6±1$^{\#}$ (n=4)
RV Systolic Pressure (mmHg)	28±3 / 7±2	38±3 / 10±1	27±2$^{\#}$ / 7±1	29±1 / 6±0 (n=4)
MPA Pressure (sys / dia, mmHg)	29±2 / 14±2	38±3 / 17±2	25±1$^{\#}$ / 13±0	28±1 / 13±2 (n=4)
RPA Pressure (sys / dia, mmHg)	27±2 / 15±2	37±2 / 18±2	25±2 / 14±1	24±2$^{\#}$ / 13±1 (n=4)
LPA Pressure (sys / dia, mmHg)	28±1 / 17±1	15±4* / 13±4	23±2 / 14±1	22±2 / 13±2 (n=4)
Stenosis/Stent Pressure Gradient (mmHg)	1±2	23±3*	1±1$^{\#}$	6±1 (n=4)
PCWP (mmHg)	10±1	11±3	8±1	7±1 (n=4)

* $p<0.05$ vs sham control, $^{\#}$ $p<0.05$ vs LPAS control

Table 1: Hemodynamics and PBF at 20-weeks for all groups

Table 2: Left lung histopathology

	Sham (n=4)	LPAS (n=4)	Delayed Intervention (n=5)	Early Intervention (n=5)
Medial Wall Thickness (%)	15±5	23±2	15±3	15±2
Alveolar Density (1,000 / mm^3)	2.10±0.43	1.36±0.14	1.43±0.11	1.86±0.34
Septal Abnormalities (1-4)	1.0±0.0	3.5±0.1*	3.2±0.2	2.6±0.3
Bronchovascular Abnormalities (1-4)	2.0±0.0	3.2±0.0*	3.1±0.2*	2.5±0.2
Interstitial Inflammation (1-4)	1.5±0.2	2.2±0.3	1.5±0.2	1.4±0.2
Alveolar Metaplasia/Attenuation (1-4)	1.0±0.0	1.6±0.2*	1.1±0.1	1.2±0.1

* $p<0.05$ vs sham control, # $p<0.05$ vs LPAS control

Table 2: Left lung histopathology